Small-Size and High-Isolation MIMO Antenna for WLAN

Zhejun Jin, Jong-Hyuk Lim, and Tae-Yeoul Yun

A small-sized (15 mm×30 mm) planar monopole MIMO antenna that offers high-isolation performance is presented in this letter. The antenna is miniaturized using inductive coupling within a meander-line radiator and capacitive coupling between a radiator and an isolator. High isolation is achieved by a T-shaped stub attached to the ground plane between two radiators, which also contributes to the small size using a folded structure and the capacitive coupling with radiators. The proposed antenna operates for the WLAN band within 2.4 GHz to 2.483 GHz. The measured isolation (S_{21}) is about −30 dB, and the envelope correlation coefficient is less than 0.1.

Keywords: Diversity, envelop correlation coefficient, isolation, MIMO, WLAN.

I. Introduction

A critical requirement of MIMO systems is to simultaneously accomplish good isolation and compact size. In reality, some electromagnetic couplings among antenna elements are inevitable even though each individual antenna element is configured to provide an independent signal path by minimizing correlations with other neighboring elements. In addition, closely-packed antennas are likely to be correlated, which gives rise to even worse isolation [1].

Several techniques [2]-[4] for achieving high port isolation have been investigated to reduce unwanted mutual coupling between antenna elements by preventing the occurrence of traveling waves from one to the other. To improve high port isolation, a mushroom-like electromagnetic band-gap [2], a defected ground system [3], and a ground plane modification [4] were utilized. Furthermore, relatively compact antennas [5], [6] have proven to provide extra isolation enhancement with a distance of less than 0.1 wavelengths between two inverted-F antennas.

All of the structures discussed above [2]-[6] occupy large areas or have modified system ground planes with slits or slots. Thus, these approaches are not applicable for limited cases or packages, which have a very small interior area. In this letter, we propose a compact MIMO antenna in which a folded T-shaped stub is inserted between meandered planar monopole antennas.

II. Antenna Design

The geometry and dimensions of the proposed configuration are depicted in Fig. 1. The top view includes two meandered monopoles with a gamma matching and a folded T-shaped stub (that is, isolator) between radiators. Each antenna element is connected to the ground plane by a shorting pin and fed by a 50-Ω SMA coaxial probe. The antenna is printed on an FR4 substrate with a relative permittivity (ε_r) of 4.7, a loss tangent ($\tan\delta$) of 0.018, and a thickness of 0.8 mm.

The operating frequency of the antenna element is approximated by

$$f_r = \frac{v_p}{4(W + L - \Delta L_m + \Delta L_c)}, \quad (1)$$

where f_r is the resonant frequency, W and L are the width and length of the meander radiator, respectively, and v_p is the phase velocity considering the dielectric substrate. ΔL_m is the

Manuscript received Mar. 3, 2011; revised May 18, 2011; accepted May 31, 2011.

This research was supported by the Ministry of Knowledge Economy (MKE), Rep. of Korea, under the Information Technology Research Center (ITRC) support program supervised by the National IT Industry Promotion Agency (NIPA) (NIPA-2011-C1090-1111-0007).

Zhejun Jin (phone: +82 2 2220 0371, kimcz@hanyang.ac.kr), Jong-Hyuk Lim (lure2you@hanyang.ac.kr), and Tae-Yeoul Yun (corresponding author, taeyeoul@hanyang.ac.kr) are with the Department of Electronic Engineering, Hanyang University, Seoul, Rep. of Korea.

http://dx.doi.org/10.4218/etrij.12.0211.0083

reduction length caused by the mutual inductance owing to the opposite current flows on the meander line [7], and ΔL_c is the extension length due to the capacitive coupling between the radiator and isolator [5]. Therefore, antenna miniaturization requires a small ΔL_m and a large ΔL_c. Although the radiator structure requires the meandering to shrink antenna size, it is necessary for the meander line to minimize the mutual inductance (ΔL_m) and thus to expand the line gap to be as large as possible. In addition, the meander line is close to the T-shaped stub to increase the capacitive coupling (ΔL_c).

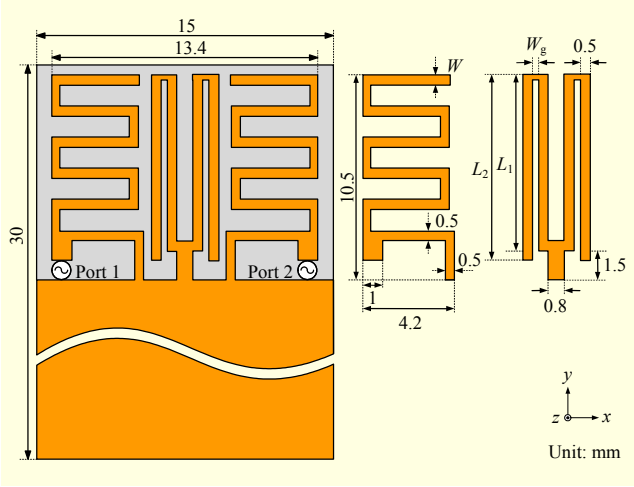

Fig. 1. Proposed miniaturized MIMO antenna.

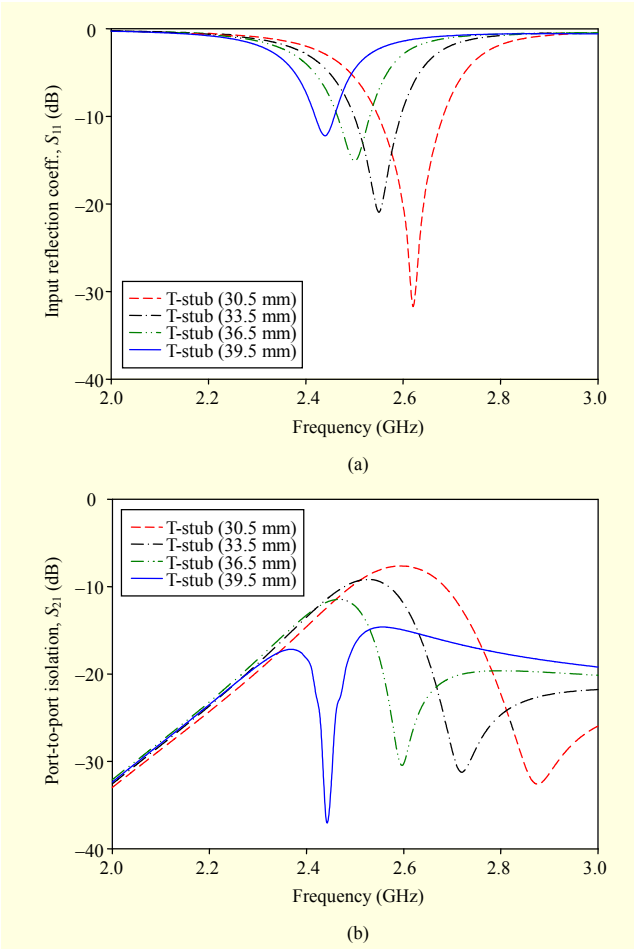

Fig. 2. *S*-parameters with different isolator lengths: (a) input reflection coefficient (S_{11}) and (b) port-to-port isolation (S_{21}).

Figure 2 shows the input reflection coefficient (S_{11}) and the port-to-port isolation (S_{21}) for a parametric analysis of the total length of a T-shaped stub. The resonance frequencies for S_{11} and S_{21} shift to lower values when the length increases. Since radiators are very close to the isolator, the optimization of the port-to-port isolation (that is, the change of the isolator's length) shifts the antenna's operating frequency, which explains the variation in capacitive coupling (ΔL_c) between the radiator and isolator.

The T-shaped stub located in the center of a MIMO antenna system can suppress direct coupling between two antenna elements. When the MIMO antenna system is in operation, the folded T-shaped stub presents an alternative coupling current path, allowing the current to flow through the arms of the stub instead of letting the coupling field appear in the other side. This coupling block phenomenon is illustrated in Fig. 2(b). The port-to-port isolation (S_{21}) is strongly dependent on the length of the stub, obeying the quarter wavelength ($\lambda/4$) rule of resonance frequency. The gap W_g (see Fig. 1) affects the electrical length caused by the mutual coupling between L_1 (inner stub) and L_2 (outer stub). Therefore, the length of the T-shaped stub is substantially longer than $\lambda/4$ of the resonance frequency.

III. Experimental Results and Discussion

In order to investigate the effects of the T-shaped stub on isolation, the following aspects were analyzed: surface current distributions on the radiators, the isolation stub, and the ground plane, all shown in Figs. 3(a) and 3(b). The radiators 1 (left) and 2 (right) are set as excited and terminated with 50 Ω, respectively. Figure 3(a) shows the poor performance of the

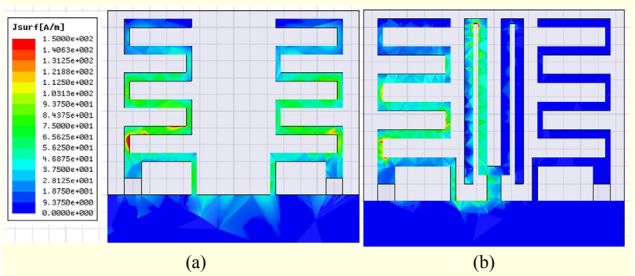

Fig. 3. Surface current distributions (port 1 excited): (a) without isolator and (b) with isolator.

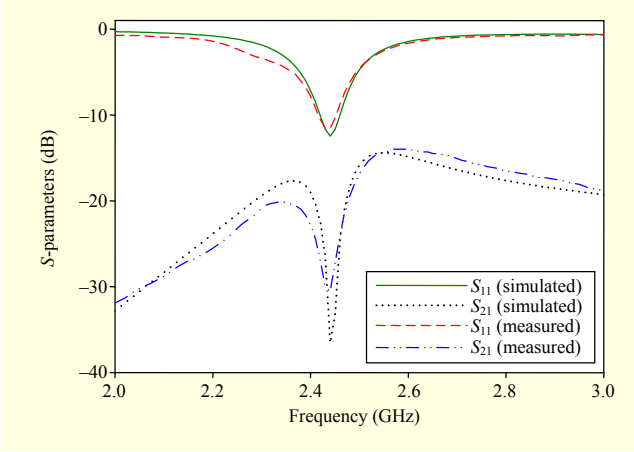

Fig. 4. Simulated and measured *S*-parameters.

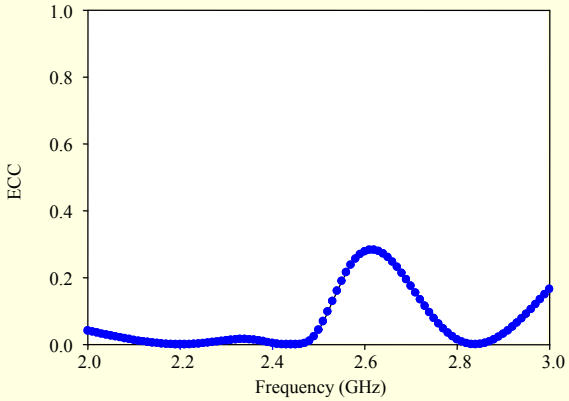

Fig. 6. Measured ECC of proposed MIMO antenna.

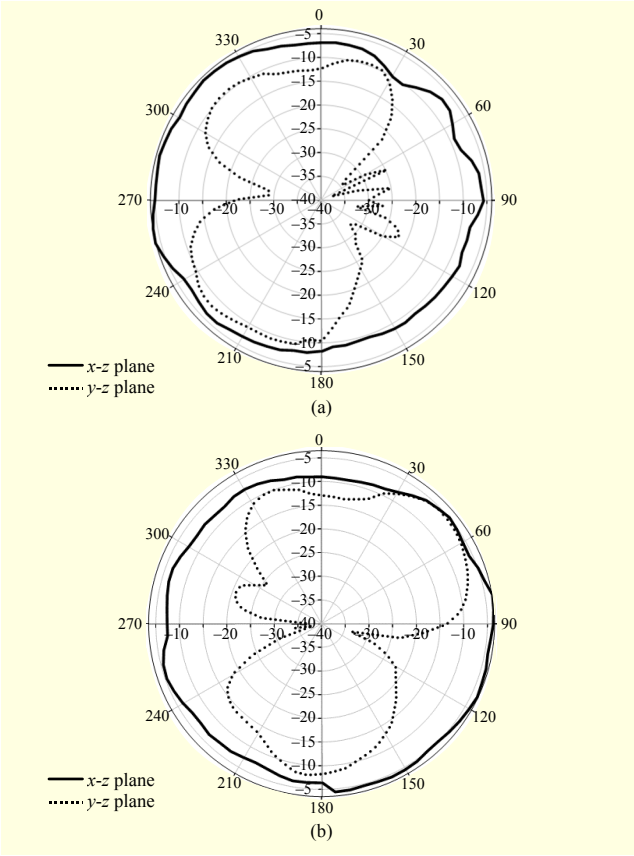

Fig. 5. Measured radiation patterns of proposed MIMO antenna: (a) antenna 1 and (b) antenna 2.

port-to-port isolation without the T-shaped stub. Figure 3(b), simulated with the isolator, shows that the surface current distributions in radiator 2 are significantly decreased.

As shown in Fig. 4, the measured *S*-parameters agree very well with the simulation. The proposed antenna has an input reflection coefficient (S_{11}) of less than –7 dB from 2.4 GHz to 2.48 GHz and a high isolation (S_{21}) with a minimum value of –30 dB.

Figure 5 plots the radiation patterns for the proposed MIMO antenna on the *x*-*z* and *y*-*z* planes at 2.44 GHz. The measured peak gain is –4 dBi, and the efficiency is 39.08%, a small value due to the small antenna size and also the large coupling between the radiator and isolator.

When considering antenna diversity and MIMO systems, the envelope correlation coefficient (ECC) is an important parameter within communication systems. A simple formulation for computing the ECC from the *S*-parameter is presented [1]. The ECC of two antennas is given by

$$\rho_{12} = \frac{\left|S_{11}^{*}S_{12} + S_{21}^{*}S_{22}\right|^{2}}{(1-\left|S_{11}\right|^{2}-\left|S_{21}\right|^{2})(1-\left|S_{22}\right|^{2}-\left|S_{12}\right|^{2})}. \quad (2)$$

The obtained ECC, shown in Fig. 6, is lower than 0.1 from the measured *S*-parameters and is sufficient for MIMO applications.

IV. Conclusion

The proposed MIMO antenna was miniaturized using the mutual inductance of a meander-line antenna as well as the capacitive coupling between an antenna element and an isolator. Port-to-port isolation was also improved by the isolator of a folded T-shaped stub located between two antenna elements, resulting in an excellent S_{21} and envelope correlation coefficient. Simulated and measured results confirmed that the proposed antenna should be useful for very limited-size MIMO antenna systems.

References

[1] S. Blanch, J. Romeu, and I. Corbella, "Exact Representation of Antenna System Diversity Performance from Input Parameter

Description," *IET Electron. Lett.*, vol. 39, no. 9, May 2003, pp. 705-707.

[2] F. Yang and Y. Rahmat-Samii, "Microstrip Antennas Integrated with Electromagnetic Band-Gap (EBG) Structures: A Low Mutual Coupling Design for Array Applications," *IEEE Trans. Antennas Propag.*, vol. 51, no. 10, Oct. 2003, pp. 2936-2946.

[3] F.G. Zhu, J.D. Xu, and Q. Xu, "Reduction of Mutual Coupling between Closely-Packed Antenna Elements Using Defected Ground Structure," *IET Electron. Lett.*, vol. 45, no. 12, July 2009, pp. 601-602.

[4] K.J. Kim and K.H. Ahn, "The High Isolation Dual-Band Inverted F Antenna Diversity System with the Small N-Section Resonators on the Ground Plane," *Microw. Opt. Technol. Lett.*, vol. 49, no. 3, Mar. 2007, pp. 731-734.

[5] A.C.K. Mak, C.R. Rowell, and R.D. Murch, "Isolation Enhancement between Two Closely Packed Antennas," *IEEE Trans. Antennas Propag.*, vol. 56, no. 11, Nov. 2008, pp. 3411-3419.

[6] S. Zhang, J. Xiong, and S. He, "MIMO Antenna System of Two Closely-Positioned PIFAs with High Isolation," *IET Electron. Lett.*, vol. 45, no. 15, July 2009, pp. 771-773.

[7] T.S. Yoon, W.S. Cho, and C.O. Kim, "Fabrication of Meander and Spiral Type Micro Inductors," *J. Mater. Sci. Technol.*, vol. 16, no. 2, Oct. 2000, pp. 236-237.